Electrophysiologic Characterization of Developing Human Embryonic Stem Cell-Derived Photoreceptor Precursors

Revital Schick,[1] Nairouz Farah,[1] Amos Markus,[1] Alon Korngreen,[2] and Yossi Mandel[1]

[1]School of Optometry and Visual Science, Faculty of Life Science and Bar-Ilan Institute for Nanotechnology and Advanced material (BINA), Bar-Ilan University, Ramat-Gan, Israel
[2]Faculty of Life Science and The Leslie and Susan Gonda Multidisciplinary Brain Research Center, Bar-Ilan University, Ramat-Gan, Israel

PURPOSE. Photoreceptor precursor cells (PRPs) differentiated from human embryonic stem cells can serve as a source for cell replacement therapy aimed at vision restoration in patients suffering from degenerative diseases of the outer retina, such as retinitis pigmentosa and AMD. In this work, we studied the electrophysiologic maturation of PRPs throughout the differentiation process.

METHODS. Human embryonic stem cells were differentiated into PRPs and whole-cell recordings were performed for electrophysiologic characterization at days 0, 30, 60, and 90 along with quantitative PCR analysis to characterize the expression level of various ion channels, which shape the electrophysiologic response. Finally, to characterize the electrically induced calcium currents, we employed calcium imaging (rhod4) to visualize intracellular calcium dynamics in response to electrical activation.

RESULTS. Our results revealed an early and steady presence (approximately 100% of responsive cells) of the delayed potassium rectifier current. In contrast, the percentage of cells exhibiting voltage-gated sodium currents increased with maturation (from 0% to almost 90% of responsive cells at 90 days). Moreover, calcium imaging revealed the presence of voltage-gated calcium currents, which play a major role in vision formation. These results were further supported by quantitative PCR analysis, which revealed a significant and continuous (3- to 50-fold) increase in the expression of various voltage-gated channels concomitantly with the increase in the expression of the photoreceptor marker CRX.

CONCLUSIONS. These results can shed light on the electrophysiologic maturation of neurons in general and PRP in particular and can form the basis for devising and optimizing cell replacement-based vision restoration strategies.

Keywords: photoreceptor precursors, stem cells, cell replacement therapy, voltage sensitive ion channels

Degenerative diseases of the outer retina, such as retinitis pigmentosa (RP) and AMD are a leading cause of blindness in the Western world.[1] They are characterized by the loss of the sensory cells of the retina, the photoreceptors, whereas the inner layers relaying the signals to the brain are left relatively intact.[2,3] Photoreceptor transplantation offers a promising strategy for vision restoration in patients suffering from these diseases.[4] Differentiation of human embryonic stem cells (hESCs) and induced pluripotent stem cells into retinal cells present an expandable and renewable source of cells for transplantation. However, varying degrees of success have been reported of differentiation toward photoreceptors and photoreceptor precursors (PRPs), as well as varying degrees of survival of the transplanted cells in animal models.[5–9] The development of photoreceptors and other retinal cell types from ESC has been extensively studied in an effort to mimic the natural differentiation of photoreceptors.[10–12] Some studies focused on exploring the sequential development of the phototransduction machinery, by measuring the continuously increasing expression of various phototransduction-related proteins (e.g., rhodopsin, recoverin, and phosphodiesterase).[6,10,13,14] Other studies focused on investigating the structural integration and synaptic formation of the transplanted cells with the host retina,[15] which is a challenge in the degenerated retina.[4] Recent reports have shown that the majority of the presumed synaptic formations are actually manifestations of cellular material transfer.[16,17]

Notwithstanding the extensive research on the gradual functional maturation of the differentiating photoreceptors and specifically light-sensitivity function maturation and anatomic integration in the host retina, little is known about the electrophysiologic maturation of the developing cells throughout the maturation process. The relatively few

available reports on the electrophysiology of stem cells specifically differentiated to PR or PRP[6,14,18–20] were performed at a relatively late stage of the differentiation process with the aim of demonstrating the resemblance between electrophysiologic responses observed in differentiated cells and mature photoreceptors. One report studying early developing retinal neurons[21] focused on spiking retinal ganglion cell-like cells, whereas presumptively nonspiking cells were not studied.

The aim of the present study was to thoroughly characterize the electrophysiologic properties of cells differentiated from hESC toward PRP, at various time points throughout the differentiation process and to simultaneously investigate the expression and functional maturation of the various ion channels.

In this study, we differentiated hESC into PRPs following a protocol recently optimized by our group.[22] We patch clamped the cells at days 0 (hESC), 30, 60, and 90 and performed an electrophysiologic characterization of the cells. As an additional measure of characterizing the differentiated cells, we investigated the expression level of various voltage-gated ion channels throughout the differentiation process using quantitative PCR analysis. We observed that derived PRPs present both voltage-sensitive Na^+ and K^+ currents as early as 30 days and that the percentage of cells presenting inward voltage-sensitive sodium currents increases throughout the maturation process, in parallel with the increase in the expression of Crx, a specific PRP marker. The electrophysiology results were in agreement with the dynamics of the expression level of the various ion channels. Our results shed light on the functional properties of a developing PRP and may aid in optimizing cell replacement-based vision restoration strategies.

Methods

Human ESC Culture

Human ESC (US National Stem Cell Bank [WA09]) were grown on mitomycin-C inactivated STO cells (a murine line derived from embryonic fibroblasts)[23] in NutriStem hPSC XF Culture Medium (Biological Industries, Beit HaEmek, Israel, 05-100-1A), supplemented with 0.5% penicillin, streptomycin, and amphotericin (Biological Industries, 03-033-1B). The medium was replaced every other day, and the cells were passaged once a week.

PRP Differentiation Protocol

To induce PRP differentiation, we used a protocol recently optimized by our group showing about 80% yield in generating PRP expressing the Crx[22] transcription factor. Briefly, agarose microwells were prepared using MicroTissues 3D Petri Dish micro-mold (Sigma-Aldrich, Rehovet, Israel, Z764051) following the manufacturer's instructions. The hESCs were detached using 0.05% trypsin (Biological Industries, 03-053-1B) and seeded in agarose microwells (9000 cells per well) in a differentiation medium containing GMEM (Gibco, Grand Isle, NY, 11710035) supplemented with 20% knockout serum replacement (Gibco, 10828028), 0.1 mM, nonessential amino acids (Biological Industries, 01-340-1B), 1 mM pyruvate (Biological Industries, 03-042-1B), 0.1 mM 2-mercaptoethanol (Sigma-Aldrich, M7522), and 1% penicillin-streptomycin-amphotericin B solution. Next, 20 mM Y-27632 (TOCRIS, Bristol, UK, 1254),

and 3 mM IWR1e (TOCRIS, 3532) were added up to day 12 and 0.1% Matrigel (GFR, BD Biosciences, San Jose, CA, FAL354230) was added from day 2. From day 12, 10% fetal bovine serum (Biological Industries, 04-127-1A) was added. From day 15 onward, 3 µM CHIR99021 (TOCRIS, 4423/10), and 100 nM SAG (TOCRIS, 4366) were added to the medium. From day 30 onward, additional growth factors were added to the medium to enhance differentiation: retinoic acid 0.5 mM (Sigma Aldrich Israel, R2625), Activin A 10 ng/mL (PeproTech, 120-14E-10), Triiodothyronine(T3) 40 µg/mL (Sigma Aldrich Israel, T2877) and Taurine 20 mM (Sigma Aldrich, Israel, T0625).

To validate the successful generation of PRP in the current set of experiments we performed FACS analysis to quantify Crx expression, which verified the high yield of the differentiation protocol (up to 95% Crx; see Supplementary Figure 1A, B)

Quantitative PCR Analysis

To investigate the time dynamics of the expression levels of various membranal channels throughout the maturation process, RNA was extracted from PRP cells at 3 time points during the differentiation from hESC: 30, 60, and 90 days and from undifferentiated hESC (H9) using the Gene Elute Mammalian Total RNA Miniprep Kit (Sigma-Aldrich, Israel, RTN70) according to the manufacturer's instructions. RT-PCR was performed on RNA extracted from the cells ,which was synthesized to cDNA using MLV reverse transcriptase, (Promega, Madison, WI, M1701). Quantitative PCR analysis was then performed using PerfeCTa SYBR Green FastMix (Quantabio, Beverly, MA, 95074-250). Here we focused on investigating the gene expression of a number of ion channels known to be expressed in mature photoreceptors, namely, NaV1.2 (SCN2A), Kv2.1 (KCNB1), Kv8.2 (KCNV2), CaV1.3 (CACNA1D), CaV1.4 (CACNA1F) plasma membrane Ca^{2+} ATPase, and hyperpolarization-activated cyclic nucleotide–gated channel 1 (HCN1).

The increase in the expression level of the gene of interest was compared to glyceraldehyde 3-phosphate dehydrogenase and normalized to the expression level of undifferentiated cells (hECs). The corresponding primers of the genes of interest are listed in the Table.

Electrophysiologic Recording

Undifferentiated hESC and 30-, 60-, and 90-day-old PRP were seeded on matrigel-coated coverslips. The coverslips were incubated at 37°C and were allowed a recovery period of at least 2 days before being transferred to the recording chamber of an upright microscope (Slicescope 6000 Scientifica, Uckfield, UK) for patch clamp recording. The chamber contained an extracellular solution consisting of: NaCl (119 mM); KCl (2.5 mM); MgCl2 (2 mM); HEPES (25 mM); CaCl2, (2 mM); and D-glucose (30 mM). A glass capillary (WPI 1.2 mm outer diameter/0.9 mm inner diameter), into which a silver wire (A-M-Systems Bare silver wire 0.010") was inserted, was pulled (PC-10, Narishige, Tokyo, Japan) to an impedance range of 4 to 8 MΩ and filled with an intracellular solution consisting of: K gluconate (125 mM); KCl (20 mM); HEPES (10 mM); MgATP (4 mM); phosphocreatine (10 mM); EGTA (0.5 mM); and GTP (0.3 mM). The whole cell configuration of the patch-clamp technique was employed to investigate the various current components, with this work focusing on voltage-sensitive sodium and potassium

TABLE. Primers used in Quantitative PCR Analysis of PRP Differentiation from hESC

Gene	Forward Primer	Reverse Primer
GAPDH	CACATGGCCTCCAAGGAGTAA	TGAGGGTCTCTCTCTTCCTCTTGT
KCNV2	CTACCAGCTGGACTACTGCG	CACCCCGGACAGGTAGAAAT
KCNB1	ATAAGGTTGAGCCACCTGCC	GTTGCTGCGCGAATACTCTG
SCN2A	TCCCAGCAGCATGACTATCAC	ACCAAGAGCAGAAGATGGCTA
HCN1	CACCAGATTGCTGGGTGTCT	ACTGGATTAAAGCGGTGGCA
CACNA1F	CTTCCGCAACCATATTCTGGG	ACCACCAGCAGATCCAACAT
CACNAID	CAGCGAAGCAGACCCAACT	ATACGGGAGCGCCTGAAAG
TMEM16B	CGCTGGCTATCGTCTCCAAT	TGCTTTGATCTCGTACATCTCT
PMCA	TCAGCCTCCAGAAGGGGATAA	ATGACCTGACCACCCCTGAT
CRX	AGAGGGCAGGGAGCCAAATC	GCCAGTGTGTGGGGAAGAGG

GADPH, glyceraldehyde 3-phosphate dehydrogenase; pMCA, plasma membrane Ca^{2+} ATPase.

currents. The cell was held at –60 mV and voltage steps ranging from –120 mV to 70 mV with a step size of 10 mV and 200 msec width were applied. To ensure the validity of the results, the cells were randomly chosen, with the following features in common: a soma which encompasses a volume (rendering the cell easily patched) and a morphology resembling that of a differentiated cell (with a soma and presumed neural processes, similar to those reported for PRPs in the study of Meyer et al[14] 2011).

The observed electrophysiologic signals were amplified (×1) and low pass filtered (Bessel 10 kHz) (multiclamp 700 b AXON), sampled at 10 kHz and saved (Digidata, Axon).

To isolate the contribution of the voltage-gated potassium channels, tetraethylammonium (TEA), a potent blocker of delayed rectifier potassium currents, was added to the recording chamber at a final concentration of 30 mM. To isolate the contribution of the voltage-gated sodium channels, tetrodotoxin (TTX), an antagonist of the voltage-gated sodium channel, was added to the recoding chamber at a final concentration of 4 μM.

Investigation of Calcium Currents

To investigate the maturation of the calcium currents, we used the red-shifted calcium indicator Rhod4 (ab112157 Abcam, Cambridge, UK) to avoid overlap with the GFP already expressed in our cells. Toward this end, the dye was prepared following the manufacturer's instructions and the cells were then incubated in 125 μL of the prepared dye in a 0.5 mL medium for 35 minutes. To stimulate the cells, biphasic 1-msec pulses of either 5 μA or 10 μA (Isolated Pulse Stimulator Model 2100-, A-M Systems, Carlsborg, WA) were applied using an external pipette (filled with the intracellular solution described elsewhere in this article) brought to the vicinity of the cell.

The fluorescence signals were visualized using the above-described microscope equipped with a CCD camera (EXI-Blue, QImaging, Moravskoslezsky, Czech Republic) at 10 Hz. The change in the fluorescence signal from baseline (as an indicator of the change in calcium) was calculated using a customized written software (see details in Supplementary Materials).

In addition to the externally injected currents, calcium dynamics were also investigated throughout the maturation process under the voltage clamp configuration and by intracellularly applying depolarizing steps, where the cell was held at –60 mV with voltage steps in 10 mV intervals starting at 0 mV

Experimental Design and Statistical Analyses

All offline analyses were performed using MATLAB R2016a (MathWorks, Natick, MA) and Bio-Rad CFX Manager 3.1. Each patch clamp recording group consisted of either 14 to 22 cells or at least 4 cells without and with blockers respectively. Quantitative PCR analysis consisted of three repetitions for each gene of interest.

Calcium signal changes were calculated by subtracting the value of each pixel in each acquired image frame from an average frame in which no stimulus was present and then dividing by this average frame (on a pixel-by-pixel basis). The average change in fluorescence signal for a cell of interest is then calculated by averaging over the corresponding pixels.

Statistical significance was determined using either paired two-tailed *t*-test or multivariate ANOVA analysis provided by the MATLAB statistics toolbox.

RESULTS

Quantitative PCR Investigation of Ion Channel Expression Dynamics

In this study, we focused on a number of ion channels and pumps, which are known to be expressed in mature photoreceptors, namely, the voltage-gated sodium channel NaV1.2 (SCN2A); two subunits of the voltage-gated potassium channel—Kv2.1 (KCNB1) and Kv8.2 (KCNV2); subunits of the voltage-gated calcium channels CaV1.3 (CACNA1D) and CaV1.4 (CACNA1F); the plasma membrane Ca^{2+} ATPase; and the HCN1. In addition to the various ion channels, which shape the electrophysiologic response, we evaluated the expression of the cone–rod homeobox protein (Crx), which is a marker of developing photoreceptors precursors, to validate the cell type of the obtained differentiated cells.

Our results reveal a stable and significant increase in the expression of the Crx marker, up to 30-fold when comparing day 90 differentiated cells to undifferentiated hESCs throughout the maturation process (Multivariate ANOVA $P < .005$) (Fig. 1a). The results verify the differentiation of hESC into PRPs, similarly to our previous report,[22] where around 80% of the cells differentiated into PRP by day 24.

A similar significant increase (multivariate ANOVA $P < .005$) was observed in the expression level of the voltage-gated sodium channel (SCN2A), which reached a 60-fold increase at day 90 (Fig. 1b). Similarly, a mild but statistically significant increase (multivariate ANOVA $P < .05$) in the expression level of the voltage-gated potassium subunit
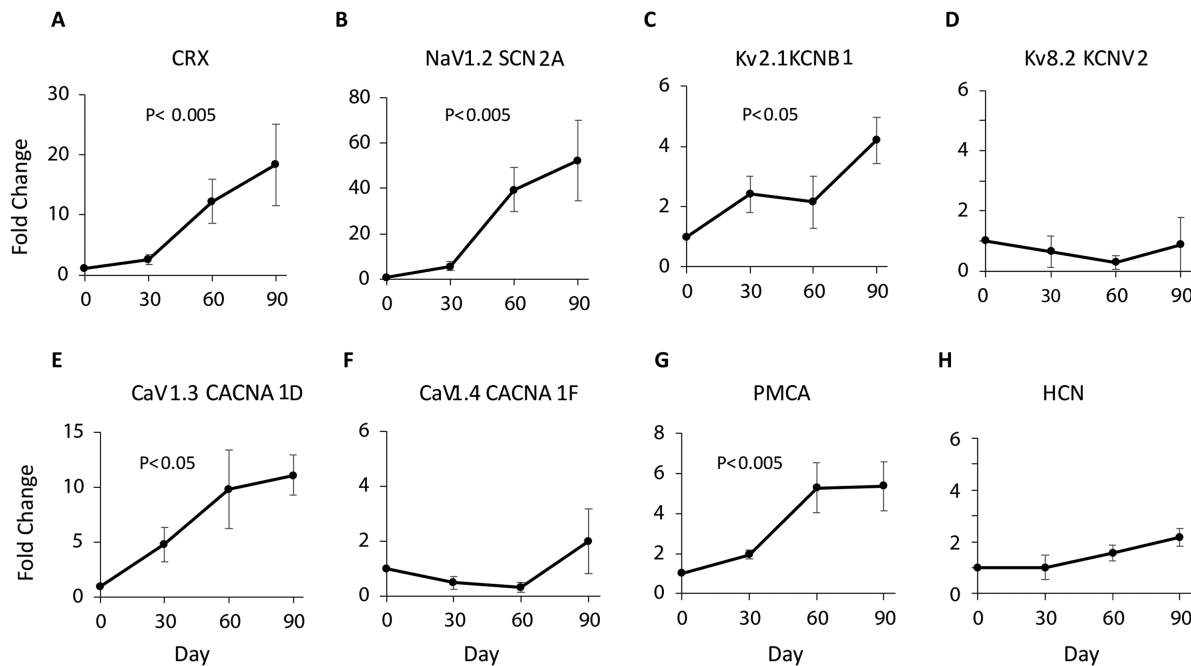
FIGURE 1. Quantitative PCR analysis of various ion channel genes throughout the maturation process of a PRP. The fold-change elevation in the expression level of Crx (**a**), NaV1.2 (SCN2A) (**b**), Kv2.1 (KCNB1) (**c**), Kv8.2 (KCNV2) (**d**), CaV1.3(CACN1D) (**e**), CaV1.4 (CACN1AF) (**f**), plasma membrane Ca^{2+} ATPase (PMCA) (**g**), and HCN (**h**) throughout the differentiation process. Three repetitions for each gene of interest.

Kv2.1 (KCNB1) was found (Fig. 1c), whereas a steady expression of the subunit Kv8.2 (KCNV2), which is known to inhibit the potassium channel Kv2,[24–26] was observed throughout the differentiation process (Fig. 1d).

A significant 11-fold elevation (multivariate ANOVA, $P < .05$) was also observed in the expression level of the voltage-gated calcium channel (CACNA1D) (Fig. 1e), which plays an important role in the synaptic signaling of the mature photoreceptor, and a steady expression in the subunit CACNA1F (Fig. 1f) was observed. An elevation in the expression level of the plasma membrane Ca^{2+}ATPase calcium pump (Fig. 1g), which is responsible for calcium extrusion in photoreceptors, was also found (multivariate ANOVA $P < .005$). Finally, the expression of HCN1 was relatively constant throughout the differentiation process (Fig. 1h).

## Electrophysiologic Characterization of Differentiating PRP

Outward Voltage Current Curve. As described in the Methods section, voltage-clamp recordings were used to investigate the contribution of the main voltage-gated ion channels to the membranal current. Representative current curves for the various differentiation time groups are presented in Figs. 2a–d.

The outward positive current, taken as the plateau of the measured current for the specific voltage step, was plotted as a function of the membrane voltage step, revealing a steady increase in the current amplitude with an activation threshold of approximately –20 mV (Fig. 2e). Moreover, the maximal current increased throughout the differentiation process, with the current at 60 mV being approximately 2.5-fold higher at 90 days differentiated cells, compared

with the hESC ($P < .001$). Multivariate ANOVA revealed that the obtained overall outward currents significantly increased throughout the maturation process (F = 30.96, $P < .001$).

Delayed Rectifier Potassium Currents. To obtain the delayed rectifier potassium currents, a major component of the voltage-gated ion currents in the photoreceptor,[27] the differentiated PRPs were patched and the currents for the previously described voltage steps were recorded (Fig. 3a, upper trace). The channel antagonist TEA was then added to the bath to a final concentration of 30 mM, leading to a complete abolition of the delayed rectifier potassium current (Fig. 3a, lower trace). In these sets of experiments, the voltage-sensitive sodium channel blocker, TTX at a final concentration of 4 μM, was also added to fully isolate the contribution of the specific potassium currents. The contribution of this specific channel was then calculated by subtracting the obtained current without the blockers from that with the blocker. The voltage–current curve of the delayed rectifier potassium currents (Fig. 3c) showed an activation potential of –20 mV, which is followed by a linear increase in the current. Although almost all cells, including the nondifferentiated hESCs (Fig. 3b), showed this characteristic potassium current I–V curve (Fig. 3c), the current amplitude gradually increased with the differentiation age (Fig. 3d) (multivariable ANOVA, F = 31.34, $P < .001$). These results are in agreement with the gradual elevation in the expression level of the voltage-gated potassium channel KCNB1 (Kv2.1) and the stable expression of the inhibiting subunit KCNV2 (Kv8.2) (Figs. 1c, d).

Voltage-Sensitive Inward Current. The second current of interest was the inward current flowing through the voltage-gated sodium channels. This current was evaluated by obtaining the amplitude of the most negative peak in the voltage current trace. To validate that these inward currents are indeed flowing through the
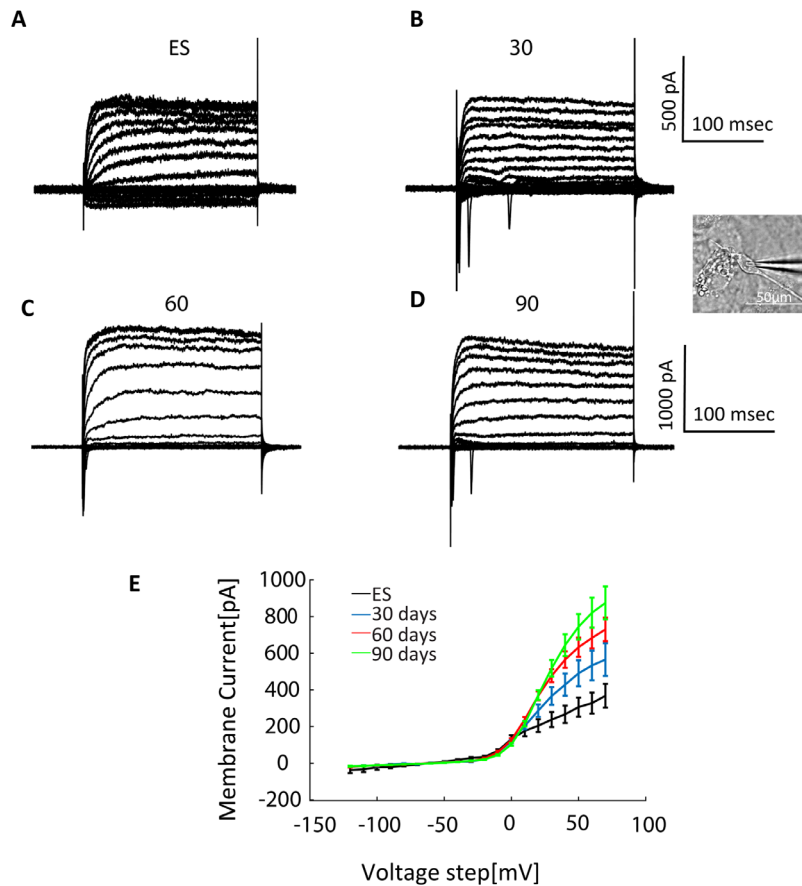
Figure 2. Electrophysiologic signals throughout the maturation process. Membrane currents for a 200-msec voltage clamp protocol applied on cells at various time points in the differentiation process. Cells were held at −60 mV and 20 voltage steps were applied (−120 mV to 70 mV). (**a**) hESC. (**b**) Thirty days, (**c**) 60 days, and (**d**) 90 days. Horizontal scale bar: 100 msec, vertical scale bar 500 pA for (**A** and **B**) and 1000 pA for (**C** and **D**), insert bright field image of a characteristic clamped cell, ×40 (scale bar = 50 μm). (**d**) The voltage–current (V–I) curve for a cell held at −60 mV with 20 voltage steps starting at −120 mV in increments of 10 mV at the various investigated time points. Error bars represent SE. (**e**) The V–I curve, for the voltage clamp protocol described in the previous section, at the various investigated time points throughout the maturation process. Number of cells used in these experiments are as follows: hESC $n = 14$; 30 days, $n = 13$; 60 days, $n = 22$; and 90 days, $n = 16$.

voltage-gated sodium channels, the relevant channel antagonist TTX was added to a final concentration of 4 μM, which completely abolished these currents (a representative trace is presented in Fig. 4a). The results revealed that these currents were not present in undifferentiated hESC but gradually appeared at a relatively early stage of the maturation process with about 50% of cells showing inward current at day 30 and almost 100% of the cells showing the current at day 90 (Fig. 4b). Interestingly, once inward currents are present in cells, the maximal current amplitude was relatively stable across all investigated differentiation age groups (Fig. 4c). The maximal obtained sodium current throughout the maturation process is presented in Fig. 4d, demonstrating that the current amplitude increases, albeit minimally, throughout the maturation process. This change, however, was not statistically significant (F = 0.6, $P = .55$ multivariate ANOVA). The gradual increase in cells presenting an inward current is in agreement with our finding of a gradual increase in the expression (Fig. 1b) of SCN2A (Na$_v$α1.2), the alpha subunit 2 of the voltage-sensitive sodium gate (Na$_v$1.2), which is found in the outer retina.[28,29]

HCN-Mediated Current (Ih). In contrast to previous studies,[14] the Ih current, mediated by the HCN channels, was not present in any of the investigated age groups. This finding was in agreement with the quantitative PCR analysis, in which no increase in the expression of HCN1 was observed (Fig. 1H). This outcome may arise from the fact that the cells used in the current study (up to 90 days of differentiation) were not mature enough to exhibit this current.

Calcium Current. The last current of interest was the calcium current. As described in the Methods section, we investigated the calcium currents at the various time points of interest by utilizing either external current injections or internal voltage steps in conjunction with calcium imaging (Fig. 5a). The elicited fluorescence change following external current injections (Fig. 5b) demonstrates the robust calcium currents upon electrical stimulation. Intracellular voltage steps elicited similar robust calcium currents, as is shown in Fig. 5c. Interestingly, all investigated age groups, including hESC, exhibited this current, with the activation threshold decreasing with maturation (multivariate ANOVA F = 3.36, $P = .027$, Fig. 5d).
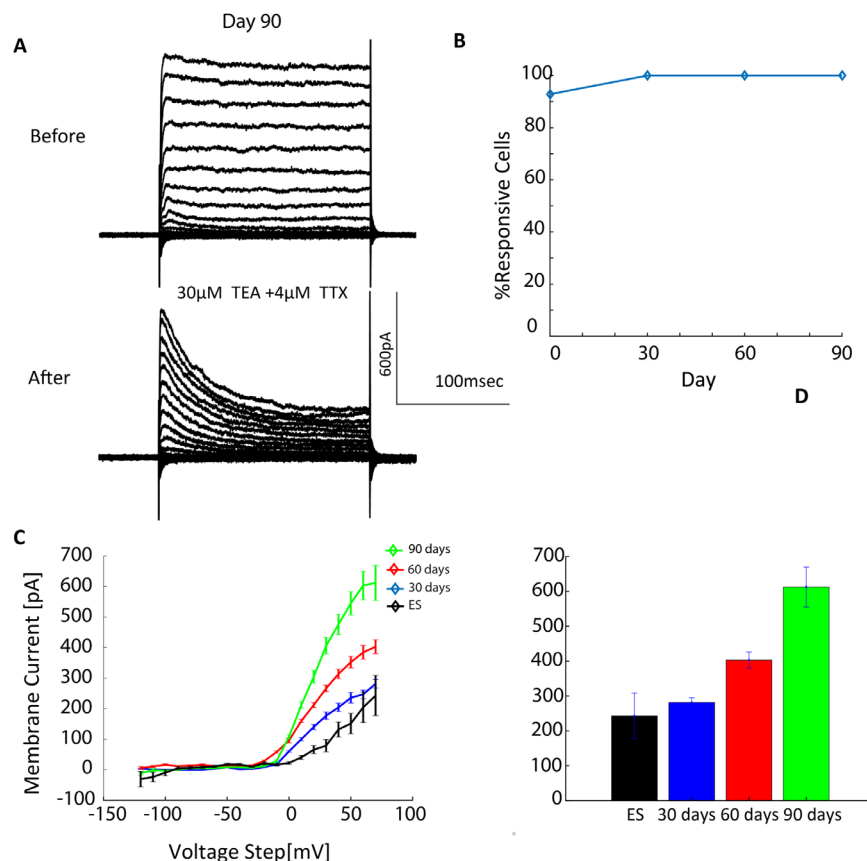
FIGURE 3. Maturation of the delayed rectifier potassium currents. (**a**) Representative signals before (*top*) and after the addition of channel blockers (*bottom*) for a cell held at −60 mV with 20 voltage steps starting at −120 mV in increments of 10 mV for a 90-day-old cell. After the addition of the voltage-gated potassium channel blocker TEA (30 mM) and the voltage-gated sodium channel blocker TTX (4μ M), all currents diminished. (**b**) The percentage of cells presenting the delayed rectifier current as a function of the differentiation day. (**c**) The delayed rectifier current V–I curve for the various investigated age groups. (**d**) The delayed rectifier potassium current at a voltage step of 70 mV for a cell held at −60 mV, at different age groups. Error bars represent the standard error. Number of cells used in these experiments are hESC, $n = 3$; 30 days, $n = 3$; 60 days, $n = 4$; and 90 days, $n = 4$.

DISCUSSION

This work presents a thorough investigation of the functional electrophysiologic maturation of PRP cells, differentiated from hESC, in terms of gene expression and electrophysiologic activity. The relatively few available reports on photoreceptors' electrophysiologic maturation focused on mature differentiated photoreceptors (e.g.,[6,18]), aiming to demonstrate the resemblance between electrophysiologic responses observed in differentiated cells and mature photoreceptors, rather than the monitoring of the functional maturation. Recently, Meyer et al. reported on the electrophysiologic responses of late-stage human induced pluripotent stem cell-derived photoreceptors.[14] In the current research, we report for the first time, to the best of our knowledge, on the functional maturation of early developing human ESC-derived PRPs in vitro.

Using our recently optimized protocol for differentiating hESC,[22] we generated PRPs expressing the Crx marker, with a relatively high yield (up to 95%) and studied their electrophysiologic maturation throughout the differentiation process up to 90 days. Interestingly, our electrophysiologic investigation revealed that the outward potassium current is observed at an early stage, with recordings from ES cells demonstrating clear outward K⁺ currents under the voltage-clamp protocol used for this work. The percentage of cells

presenting this current does not increase with maturation, with almost all investigated cells exhibiting this current. This outward current was blocked by TEA and is thus presumably mediated by delayed rectifier potassium channels, similar to Meyer et al.,[14] who reported on outward currents in photoreceptor-like cells derived from optic vesicles, with comparable measured currents (around 400 pA to 450 pA at 40 mV). The delayed rectifier currents play a major role in limiting membrane excitability[30] and are facilitated by a family of potassium channels Kv2,[31] which are modified (suppressed) by the KCNV2 (also known as KV11.1 or Kv8.2 subunit).[24–26] The ratio between the expression levels of KCNB1 (Kv2.1) and KCNV2 (Kv8.2 subunit) determines the outward potassium current in the photoreceptors[26] (with several mutations in the KCNV2 gene[32,33] being associated with cone degenerations). Thus, the gradual increase in KCNB1, accompanied by the constant KCNv2 expression observed in our developing PRPs, is in line with the gradual increase in the measured outward current. Our findings are further supported by Homma et al.,[18] who found a gradual increase in various subunits of the K⁺ channel during the postnatal retinal development.

Moreover, we observed robust voltage-sensitive inward Na⁺ currents, which were blocked by TTX. The percentage of cells expressing this current gradually increased with maturation, whereas the current amplitude was
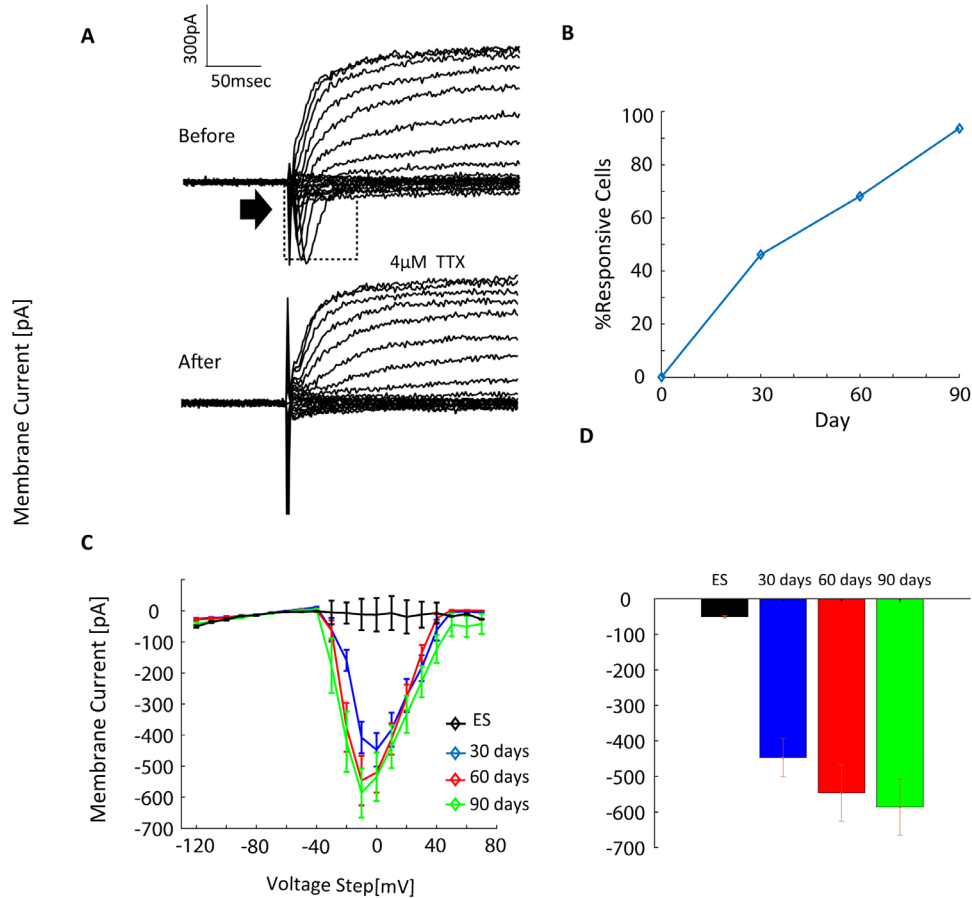
FIGURE 4. Voltage-gated sodium current maturation currents. (**a**) Representative signals before (*upper trace*) and after (*lower trace*) the addition of channel blocker (*bottom*) for a cell held at −60 mV and 20 voltage steps starting at −120 mV in increments of 10 mV for a 90-day-old cell. After the addition of the voltage-gated sodium channel blocker TTX (4 μM), all inward currents diminished. (**b**) The percentage of cells exhibiting the voltage-gated sodium current as a function of differentiation time throughout the maturation process. (**c**) The voltage-gated sodium current V–I curve for the various investigated time points. (**d**) The maximal amplitude of the voltage-gated sodium current at a voltage step of 70 mV for a cell held at −60 mV, at different age groups. Error bars represent the standard error. Number of cells used in these experiments are: hESC, $n = 14$; 30 days, $n = 6$; 60 days, $n = 15$; $n = 6$; 90 days, $n = 15$).

relatively stable. Although photoreceptors are usually considered nonspiking neurons, showing only graded potential, which is considered better for encoding sensory information,[34,35] several papers reported action potentials elicited in PR in response to depolarizing electric signals.[36–38] The inward Na$^+$ current observed in our PRPs reached a maximum of about 600 pA at −20 mV, comparable with the current characterized by Kawai et al.[37] in mature human photoreceptors.

Our results, showing an increase in the percentage of cells exhibiting voltage-dependent Na$^+$ current, are also supported by our findings of increased expression of SCN2A (Na$_v\alpha$1.2), the alpha subunit 2 of the voltage-sensitive sodium gate, which was reported in mature photoreceptors.[28,29] Copenhagen[35] suggested that the voltage-gated Na+ current can boost the initial graded potential. This finding is similar to bipolar cells, where voltage-gated sodium channels were also presumed to mediate input both directly or through GABAergic inhibitory cells.[39,40] Recently, other voltage-gated sodium channels have been reported in the retinal layers (e.g., Nav1.9), including the photoreceptors, localized mainly at the cone pedicle and the rod spherule. These currents are presumed to contribute to the

enhancement of the response to phototransduction and to the rapid depolarization of the pedicle during light adaptation and to returning the potential to the voltage range necessary for calcium-mediated glutamate release. These slowly deactivated channels were not studied in our present study and their contribution to the Na$^+$ current was not recorded because they are TTX insensitive.[41]

The third current of importance, the hyperpolarization-activated current (Ih), was not observed in our developing cells. This was further supported by the quantitative PCR results wherein the expression of HCN1 in our developing cells showed minimal or no increase. Our findings are in agreement with Homma et al.,[18] who found little expression of HCN-1 mRNA in P5 mouse retinas, but with a significant increase during maturation to adult mouse retina. The Ih currents were reported in human photoreceptors and are believed to be activated by and oppose the light-generated photoreceptors' hyperpolarization in response to bright light stimuli. This phenomenon results in an enhancement in temporal resolution[42–45] and the prevention of visual flickering by inhibiting the generation of spontaneous spikes, as suggested by Miyachi et al..[29] The fact that our PRPs did not show Ih could be explained by their relatively early
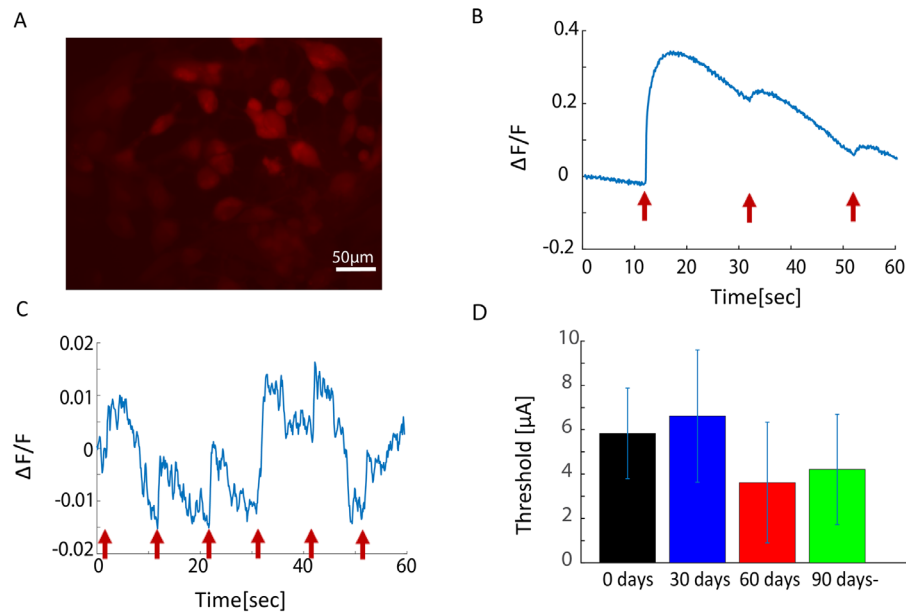
FIGURE 5. The maturation of the calcium current. (**a**) Florescence imaging of a 90-day-old cell culture stained with the calcium indicator Rhod4. (**b**) A representative trace of the induced robust calcium change. Fluorescence signal change induced by three 5 µA, 1 msec biphasic pulses in a 90-day cell. This trace highlights the presence of the highly essential voltage-gated calcium channel in our differentiated cell. (**c**) A representative trace of the induced robust change in an intracellularly activated cell (held at −60 mV, induced through voltage steps starting from 0 V in steps of 10 mV). *Red arrow* indicates stimulus onset. (**d**) The activation threshold as a function of differentiation day. Results highlight the mild yet statistically significant decrease in activation threshold throughout the maturation process ($P < .05$). Number of cells used in these experiments are: hESC, $n = 6$; 30 days, $n = 13$; 60 days, $n = 13$; 90 days, $n = 16$.

maturation, and the lack of a clear and mature inner segment where the HCN channels are localized.[18,45] To further evaluate the lh current, future studies should be performed on more mature cells (at an extended time point beyond 90 days).

Also of interest to the current study was the evaluation of calcium currents. Our results showed a robust increase in the expression of the CACNA1D gene, encoding the calcium Cav1.3 subunit.[46] The Cav1.3 channels are found in the photoreceptor's inner segment and other photoreceptor sites as well as in other cells of the retina. More important, Shi et al.[47] showed that deletion of Cav1.3 in mutant mice caused a reduction in the density of ribbon synapses in the OPL, suggesting that this protein is critical for the maintenance of the ribbon synapse.

In contrast with the robust increase in Cav1.3 (CACNA1D), we observed a stable expression of CaV1.4 (CACNA1F), which codes to the alpha-1 subunit of the voltage-gated calcium channel CaV1.4, widely found in the human photoreceptor synaptic terminals.[47–50] Mutation in this gene can cause severe loss of photoreceptor function in various diseases, such as X-lined congenital stationary night blindness[51–54] and cone–rod dystrophy,[55] and can affect synaptic maturation during retinal development.[56–59] This channel is also important for generating the ribbon synapse during maturation of the retina. The lack of increased expression in this channel is in line with the fact that the PRPs used in the current study were not mature and obviously have not yet created a synapse. In contrast, Homma et al.[18] reported an increase in the expression level of various voltage-sensitive Ca^{2+} channels in naturally developing mouse retina. Calcium response to glutamate or depolarization by K^+ solution was reported in several publications.[6,18] In our study, we investigated the calcium

response using either externally applied currents or internally applied voltage steps, revealing robust calcium changes in response to an increasing current presenting an additional aspect of the functional maturation of the differentiated cells.

Our results are also in agreement with studies reporting the electrophysiologic maturation of other neurons differentiated from human pluripotent cells. For example, Johnson et al.[60] reported on neurons differentiated from hESC, which exhibited an increase in Na^+ inward current and spontaneous activity with maturation. In contrast, similar to our findings, the transient K^+ current increased, whereas the sustained K^+ current density decreased. Yet another report showed that K^+ current increased with maturation[61] where Prè et al.[62] reported that the Na^+ current density increase was accompanied with a stable K^+ current density throughout maturation. Furthermore, our results are also in agreement with Lepski et al.,[63] who reported potassium currents recorded as early as 2 weeks in differentiation, with a gradual increase in the current density throughout the neural maturation. It is worth noting that, notwithstanding the undifferentiated cells that may have been included in our analysis, the high efficiency of the differentiation protocol indicates that the clear observed correlation between the channels gene expression dynamics and the electrophysiologic results could have been even more profound had the population been purified further validating our results. A more reliable, free of undifferentiated analysis can be obtained using reporter-labeled hESC line in which the GFP expression is controlled by CRX (e.g.[64]). Future studies should also estimate the dynamics of ionic channels development using immunochemistry staining. Thus, our findings, with the additional characterization of the various ionic channel expression dynamic over the differentiation process

can also serve as an important basis for understanding the functional differentiation of human neurons.

Finally, notwithstanding the applicability of our findings, it should be noted that the in vitro differentiation of hESC into PRP is significantly slower compared with the development of the retina during embryogenesis, where partial stratification of the retina is evident at 8 weeks after conception with photoreceptors and inner cells synapses with the outer plexiform layer already observed.[65,66] Although it is known that the fetal eye can respond to light[67] at week 26, there is lack of information regarding the functionality at the earlier stages.

CONCLUSIONS

This study presents a thorough investigation of the biophysical maturation of PRPs and sheds light on their electrophysiology. In contrast with quantitative PCR, which is a population-based characterization of cells, electrophysiologic investigations are a single cell procedure. The syngenetic combination of these two complementary characterization modalities of developing cells leads to a better and more complete understanding of the differentiation process. Electrophysiologic development is known to affect cell fate[68] as well as regulating synaptic formation in developing retinal neurons,[69] and thus may affect the integration of transplanted cells with a host tissue. Further understanding of the electrophysiologic maturation, as a complimentary to the widely used characterization by vision cycle related markers (e.g., opsins), may thus aid in understanding processes that are involved with photoreceptor integration within the host retina, which is currently a major hurdle in retinal replacement therapy strategies.

References

1. Colijn JM, Buitendijk GHS, Prokofyeva E, et al. Prevalence of age-related macular degeneration in Europe: the past and the future. *Ophthalmology*. 2017;124:1753–1763.
2. Santos A, Humayun MS, De Juan E, et al. Preservation of the inner retina in retinitis pigmentosa: a morphometric analysis. *Arch Ophthalmol*. 1997;115:511–515.
3. Humayun MS, Prince M, de Juan E, et al. Morphometric analysis of the extramacular retina from postmortem eyes with retinitis pigmentosa. *Invest Ophthalmol Vis Sci*. 1999;40:143–148.
4. Gasparini SJ, Llonch S, Borsch O, et al. Transplantation of photoreceptors into the degenerative retina: current state and future perspectives. *Prog Retin Eye Res*. 2018;69:1–37.
5. Laver CRJ, Metcalfe AL, Szczygiel L, et al. Bimodal in vivo imaging provides early assessment of stem-cell-based photoreceptor engraftment. *Eye*. 2015;29:681–690.
6. Gonzalez-Cordero A, West EL, Pearson RA, et al. Photoreceptor precursors derived from three-dimensional embryonic stem cell cultures integrate and mature within adult degenerate retina. *Nat Biotechnol*. 2013;31:741–747.
7. Santos-Ferreira T, Llonch S, Borsch O, et al. Retinal transplantation of photoreceptors results in donor–host cytoplasmic exchange. *Nat Commun*. 2016;7:13028.
8. Pearson RA, Barber AC, Rizzi M, et al. Restoration of vision after transplantation of photoreceptors. *Nature*. 2012;485:99–103.
9. Lamba DA, McUsic A, Hirata RK, et al. Generation, purification and transplantation of photoreceptors derived from human induced pluripotent stem cells. *PLoS One*. 2010;5:e8763.
10. Osakada F, Ikeda H, Mandai M, et al. Toward the generation of rod and cone photoreceptors from mouse, monkey and human embryonic stem cells. *Nat Biotechnol*. 2008;26:215–225.
11. Eiraku M, Sasai Y. Mouse embryonic stem cell culture for generation of three-dimensional retinal and cortical tissues. *Nat Protoc*. 2011;7:69–79.
12. Ikeda H, Osakada F, Watanabe K, et al. Generation of Rx+/Pax6+ neural retinal precursors from embryonic stem cells. *Proc Natl Acad Sci USA*. 2005;102:11331–11336.
13. West EL, Gonzalez-Cordero A, Hippert C, et al. Defining the integration capacity of embryonic stem cell-derived photoreceptor precursors. *Stem Cells*. 2012;30:1424–1435.
14. Meyer JS, Howden SE, Wallace KA, et al. Optic vesicle-like structures derived from human pluripotent stem cells facilitate a customized approach to retinal disease treatment. *Stem Cells*. 2011;29:1206–1218.
15. Zhong X, Gutierrez C, Xue T, et al. Generation of three-dimensional retinal tissue with functional photoreceptors from human iPSCs. *Nat Commun*. 2014;5:4047.
16. Pearson RA, Gonzalez-Cordero A, West EL, et al. Donor and host photoreceptors engage in material transfer following transplantation of post-mitotic photoreceptor precursors. *Nat Commun*. 2016;7:13029.
17. Nickerson PEB, Ortin-Martinez A, Wallace VA. Material exchange in photoreceptor transplantation: updating our understanding of donor/host communication and the future of cell engraftment science. *Front Neural Circuits*. 2018;12:17.
18. Homma K, Okamoto S, Mandai M, et al. Developing rods transplanted into the degenerating retina of Crx-knockout mice exhibit neural activity similar to native photoreceptors. *Stem Cells*. 2013;31:1149–1159.
19. Hallam D, Hilgen G, Dorgau B, et al. Human-induced pluripotent stem cells generate light responsive retinal organoids with variable and nutrient-dependent efficiency. *Stem Cells*. 2018;36:1535–1551.
20. Deng WL, Gao ML, Lei XL, et al. Gene correction reverses ciliopathy and photoreceptor loss in iPSC-derived retinal organoids from retinitis pigmentosa patients. *Stem Cell Reports*. 2018;10:1267–1281.
21. Chen L-F, Yin ZQ, Chen S, et al. Differentiation and production of action potentials by embryonic rat retina stem cells in vitro. *Investig Ophthalmol Vis Sci*. 2008;49:5144.
22. Markus A, Shamul A, Chemla Y, et al. An optimized protocol for generating labeled and transplantable photoreceptor precursors from human embryonic stem cells. *Exp Eye Res*. 2019;180:29–38.
23. Park JH, Kim SJ, Oh EJ, et al. Establishment and maintenance of human embryonic stem cells on STO, a permanently growing cell line1. *Biol Reprod*. 2003;69:2007–2014.
24. Jorge BS, Campbell CM, Miller AR, et al. Voltage-gated potassium channel KCNV2 (Kv8.2) contributes to epilepsy susceptibility. *Proc Natl Acad Sci USA*. 2011;108:5443–5448.
25. Ottschytsch N, Raes A, Van Hoorick D, et al. Obligatory heterotetramerization of three previously uncharacterized

Kv channel -subunits identified in the human genome. *Proc Natl Acad Sci USA.* 2002;99:7986–7991.

26. Czirják G, Tóth ZE, Enyedi P. Characterization of the heteromeric potassium channel formed by Kv2.1 and the retinal subunit Kv8.2 in *Xenopus* oocytes. *J Neurophysiol.* 2007;98:1213–1222.

27. Pinto LH, Klumpp DJ. Localization of potassium channels in the retina. *Prog Retin Eye Res.* 1998;17:207–230.

28. Mojumder DK, Frishman LJ, Otteson DC, et al. Voltage-gated sodium channel alpha-subunits Na(v)1.1, Na(v)1.2, and Na(v)1.6 in the distal mammalian retina. *Mol Vis.* 2007;13:2163–2182.

29. Miyachi E, Kawai F, Ohkuma M, et al. Electrophysiological study of voltage-gated ion channels in photoreceptors and bipolar cells in the human retina. *Proc Physiol Soc. vol. Proceedings of the 37th, Physiological Society,* 2013:

30. Misonou H, Mohapatra DP, Trimmer JS. Kv2.1: a voltage-gated K+ channel critical to dynamic control of neuronal excitability. *Neurotoxicology,* vol. 26. New York: Elsevier; 2005:743–752.

31. Murakoshi H, Trimmer JS. Identification of the Kv2.1 K+ channel as a major component of the delayed rectifier K+ current in rat hippocampal neurons. *J Neurosci.* 1999;19:1728–1735.

32. Wu H, Cowing JA, Michaelides M, et al. Mutations in the gene KCNV2 encoding a voltage-gated potassium channel subunit cause "cone dystrophy with supernormal rod electroretinogram" in humans. *Am J Hum Genet.* 2006;79:574–579.

33. Robson AG, Webster AR, Michaelides M, et al. "Cone dystrophy with supernormal rod electroretinogram": a comprehensive genotype/phenotype study including fundus autofluorescence and extensive electrophysiology. *Retina.* 2010;30:51–62.

34. Juusola M, French AS. The efficiency of sensory information coding by mechanoreceptor neurons. *Neuron.* 1997;18:959–968.

35. Copenhagen D. Is the retina going digital? *Neuron.* 2001;30:303–305.

36. Ohkuma M, Kawai F, Horiguchi M, et al. Patch-clamp recording of human retinal photoreceptors and bipolar cells. *Photochem Photobiol.* 2007;83:317–322.

37. Kawai F, Horiguchi M, Suzuki H, et al. Na(+) action potentials in human photoreceptors. *Neuron.* 2001;30:451–458.

38. Kawai F, Horiguchi M, Ichinose H, et al. Suppression by an *h* current of spontaneous Na$^+$ Action potentials in human cone and rod photoreceptors. *Investig Ophthalmol Vis Sci.* 2005;46:390.

39. Smith BJ, Tremblay F, Côté PD. Voltage-gated sodium channels contribute to the b-wave of the rodent electroretinogram by mediating input to rod bipolar cell GABA(c) receptors. *Exp Eye Res.* 2013;116:279–290.

40. Zenisek D, Henry D, Studholme K, et al. Voltage-dependent sodium channels are expressed in nonspiking retinal bipolar neurons. *J Neurosci.* 2001;21:4543–4550.

41. O'Brien BJ, Caldwell JH, Ehring GR, et al. Tetrodotoxin-resistant voltage-gated sodium channels Na(v)1.8 and Na(v)1.9 are expressed in the retina. *J Comp Neurol.* 2008;508:940–951.

42. Barrow AJ, Wu SM. Low-conductance HCN1 ion channels augment the frequency response of rod and cone photoreceptors. *J Neurosci.* 2009;29:5841–5853.

43. Seeliger MW, Brombas A, Weiler R, et al. Modulation of rod photoreceptor output by HCN1 channels is essential for regular mesopic cone vision. *Nat Commun.* 2011;2:532.

44. Sothilingam V, Michalakis S, Garcia Garrido M, et al. HCN1 channels enhance rod system responsivity in the retina under conditions of light exposure. *PLoS One.* 2016;11:e0147728.

45. Kawai F, Horiguchi M, Suzuki H, et al. Modulation by hyperpolarization-activated cationic currents of voltage responses in human rods. *Brain Res.* 2002;943:48–55.

46. Snutch TP. Voltage-gated calcium channels. *Encycl Neurosci.* 2009;10:427–441.

47. Shi L, Chang JY-A, Yu F, et al. The contribution of L-type Cav1.3 channels to retinal light responses. *Front Mol Neurosci.* 2017;10:394.

48. Lee A, Wang S, Williams B, et al. Characterization of Ca$_v$ 1.4 complexes (α_1 1.4, β_2, and α_2 δ_4) in HEK293T cells and in the retina. *J Biol Chem.* 2015;290:1505–1521.

49. Baker SA, Kerov V. Photoreceptor inner and outer segments. *Curr Top Membr.* 2013;72:231–265.

50. Haeseleer F, Imanishi Y, Maeda T, et al. Essential role of Ca2+-binding protein 4, a Cav1.4 channel regulator, in photoreceptor synaptic function. *Nat Neurosci.* 2004;7:1079–1087.

51. Haeseleer F, Williams B, Lee A. Characterization of C-terminal splice variants of Cav1.4 Ca2+ channels in human retina. *J Biol Chem.* 2016;291:15663–15673.

52. Wutz K, Sauer C, Zrenner E, et al. Thirty distinct CACNA1F mutations in 33 families with incomplete type of XLCSNB and Cacna1f expression profiling in mouse retina. *Eur J Hum Genet.* 2002;10:449–456.

53. Boycott KM, Pearce WG, Bech-Hansen NT. Clinical variability among patients with incomplete X-linked congenital stationary night blindness and a founder mutation in CACNA1F. *Can J Ophthalmol.* 2000;35:204–213.

54. Hemara-Wahanui A, Berjukow S, Hope CI, et al. A CACNA1F mutation identified in an X-linked retinal disorder shifts the voltage dependence of Cav1.4 channel activation. *Proc Natl Acad Sci USA.* 2005;102:7553–7558.

55. Nakamura M, Ito S, Piao C-H, et al. Retinal and optic disc atrophy associated with a CACNA1F mutation in a Japanese family. *Arch Ophthalmol.* 2003;121:1028.

56. Kerov V, Laird JG, Joiner M, et al. α_2 δ-4 is required for the molecular and structural organization of rod and cone photoreceptor synapses. *J Neurosci.* 2018;38:3818–3816.

57. Zabouri N, Haverkamp S. Calcium channel-dependent molecular maturation of photoreceptor synapses. *PLoS One.* 2013;8:e63853.

58. Cao Y, Sarria I, Fehlhaber KE, et al. Mechanism for selective synaptic wiring of rod photoreceptors into the retinal circuitry and its role in vision. *Neuron.* 2015;87:1248–1260.

59. Liu X, Kerov V, Haeseleer F, et al. Dysregulation of Ca$_v$ 1.4 channels disrupts the maturation of photoreceptor synaptic ribbons in congenital stationary night blindness type 2. *Channels.* 2013;7:514–523.

60. Johnson MA, Weick JP, Pearce RA, et al. Functional neural development from human embryonic stem cells: accelerated synaptic activity via astrocyte coculture. *J Neurosci.* 2007;27:3069–3077.

61. Nicholas CR, Chen J, Tang Y, et al. Functional maturation of hPSC-derived forebrain interneurons requires an extended timeline and mimics human neural development. *Cell Stem Cell.* 2013;12:573–586.

62. Prè D, Nestor MW, Sproul AA, et al. A time course analysis of the electrophysiological properties of neurons differentiated from human induced pluripotent stem cells (iPSCs). *PLoS One.* 2014;9:e103418.

63. Lepski G, Maciaczyk J, Jannes CE, et al. Delayed functional maturation of human neuronal progenitor cells in vitro. *Mol Cell Neurosci.* 2011;47:36–44.

64. Collin J, Mellough CB, Dorgau B, et al. Using zinc finger nuclease technology to generate CRX-reporter human embryonic stem cells as a tool to identify and study the

emergence of photoreceptors precursors during pluripotent stem cell differentiation. *Stem Cells*. 2016;34:311–321.

65. Hendrickson A. Development of retinal layers in prenatal human retina. *Am J Ophthalmol*. 2016;161:29–35.e1.

66. Smyth CN. Exploratory methods for testing the integrity of the foetus and neonate. *BJOG*. 1965;72:395–396.

67. Polishuk WZ, Laufer N, Sadovsky E. Fetal reaction to external light (Hebrew). *Harefuah*. 1975;89:395–396.

68. Zhang LI, Poo MM. Electrical activity of neural circuits. *Nat Neurosci*. 2001;4(Suppl.):1207–1214.

69. Johnson RE, Kerschensteiner D. Retrograde plasticity and differential competition of bipolar cell dendrites and axons in the developing retina. *Curr Biol*. 2014;24:2301–2306.